

Exotic $\mu^- - e^-$ conversion in nuclei and R-parity violating supersymmetry

Amand Faessler^a, T.S. Kosmas^b, Sergey Kovalenko^{c,1} and J.D. Vergados^b

^a*Institut für Theoretische Physik der Universität Tübingen, D-72076 Tübingen, Germany*

^b*Division of Theoretical Physics, University of Ioannina GR-45110 Ioannina, Greece*

^c*Departamento de Física, Universidad Técnica Federico Santa María, Casilla 110-V, Valparaíso, Chile*

Abstract

The flavor violating $\mu^- - e^-$ conversion in nuclei is studied within the minimal supersymmetric standard model. We focus on the R-parity violating contributions at tree level including the trilinear and the bilinear terms in the superpotential as well as in the soft supersymmetry breaking sector. The nucleon and nuclear structure have consistently been taken into account in the expression of the $\mu^- - e^-$ conversion branching ratio constructed in this framework. We have found that the contribution of the strange quark sea of the nucleon is comparable with that of the valence quarks. From the available experimental data on $\mu^- - e^-$ conversion in ^{48}Ti and ^{208}Pb and the expected sensitivity of the MECO experiment for ^{27}Al we have extracted new stringent limits on the R-parity violating parameters.

PACS: 12.60.Jv, 11.30.Er, 11.30.Fs, 23.40.Bw

KEYWORDS: Lepton flavor violation, exotic $\mu - e$ conversion in nuclei, supersymmetry, R-parity violation, muon capture.

¹On leave of absence from the Joint Institut for Nuclear Research, Dubna, Russia

1 Introduction

The lepton flavor violating process of neutrinoless muon-to-electron ($\mu - e$) conversion in a nucleus, represented by

$$\mu^- + (A, Z) \longrightarrow e^- + (A, Z)^*, \quad (1)$$

is an exotic process very sensitive to a plethora of new-physics extensions of the standard model (SM) [1]-[5]. In addition, experimentally it is accessible with incomparable sensitivity. Long time ago Marciano and Sanda [1] has proposed it as one of the best probes to search for lepton flavor violation beyond the standard model. Recently, in view of the indications for neutrino oscillations in super-Kamiokande, solar neutrino and LSND data, new hope has revived among the experimentalists of nuclear and particle physics to detect other signals for physics beyond the SM. A prominent probe in this spirit is this exotic process (1).

The fact that the upper limits on the branching ratio of the $\mu^- - e^-$ conversion relative to the ordinary muon capture,

$$R_{\mu e^-} = \Gamma(\mu^- \rightarrow e^-)/\Gamma(\mu^- \rightarrow \nu_\mu), \quad (2)$$

offer the lowest constraints compared to any purely leptonic rare process motivated a new $\mu^- - e^-$ conversion experiment, the so called MECO experiment at Brookhaven [6, 7, 8], which got recently scientific approval and is planned to start soon. The MECO experiment is going to use a new very intense μ^- beam and a new detector operating at the Alternating Gradient Synchrotron (AGS). The basic feature of this experiment is the use of a pulsed μ^- beam to significantly reduce the prompt background from π^- and e^- contaminations. For technical reasons the MECO target has been chosen to be the light nucleus ^{27}Al . Traditionally the $\mu - e$ conversion process was searched by employing medium heavy (like ^{48}Ti and ^{63}Cu) [9, 10] or very heavy (like ^{208}Pb and ^{197}Au) [9, 11, 12] targets (for a historical review on such experiments see Ref. [13]). The best upper limits on $R_{\mu e^-}$ set up to the present have been extracted at PSI by the SINDRUM II experiments resulting in the values

$$R_{\mu e^-} \leq 6.1 \times 10^{-13} \quad \text{for } ^{48}\text{Ti target [9],} \quad (3)$$

$$R_{\mu e^-} \leq 4.6 \times 10^{-11} \quad \text{for } ^{208}\text{Pb target [10].} \quad (4)$$

(at 90% confidence level). The experimental sensitivity of the Brookhaven experiment is expected to be roughly

$$R_{\mu e^-} \leq 2 \times 10^{-17} \quad \text{for } ^{27}\text{Al target [6, 7]} \quad (5)$$

i.e. three to four orders of magnitude below the existing experimental limits.

It is well known that the process (1) is a very good example of the interplay between particle and nuclear physics attracting significant efforts from both sides. The underlying nuclear physics of the $\mu - e$ conversion has been comprehensively studied in Refs. [13]-[16]. From the particle physics point of view, processes like $\mu - e$ conversion, is forbidden in the SM by muon and electron quantum number conservation. Therefore it has long been recognized as an important probe of the flavor changing neutral currents and possible physics beyond the SM [1]-[5].

On the particle physics side there are many mechanisms of the $\mu - e$ conversion constructed in the literature (see [5, 17, 18, 19] and references therein). All these mechanisms fall into two different categories: photonic and non-photonic. Mechanisms from different categories significantly differ from the point of view of the nucleon and nuclear structure calculations. This stems from the fact that they proceed at different distances and, therefore, involve different details of the structure. The long-distance photonic mechanisms are mediated by the photon exchange between the quark and the $\mu - e$ -lepton currents. These mechanisms resort to the lepton-flavor non-diagonal electromagnetic vertex which is presumably induced by the non-standard model physics at the loop level. The contributions to the $\mu - e$ conversion via virtual photon exchange exist in all models which allow $\mu \rightarrow e\gamma$ decay. The short-distance non-photonic mechanisms contain heavy particles in intermediate states and can be realized at the tree level, at the 1-loop level or at the level of box diagrams.

The non-photonic mechanisms are mediated by various particles in intermediate states such as W, Z -bosons [1]-[5], Higgs bosons [2, 5], supersymmetric particles (squarks, sleptons, gauginos, higgsinos etc.) with and without R -parity conservation in the vertices.

In the supersymmetric (SUSY) extensions of the SM with conserved R -parity (R_p SUSY) $\mu^- - e^-$ conversion has been studied in Refs. [16, 20]. In this case the SUSY contributions appear only at the loop or box level and, therefore, they are suppressed by the loop factor. The situation is different in the SUSY models with R -parity non-conservation (\tilde{R}_p SUSY). In this framework there exist the tree level non-photonic contributions [17, 19] and the 1-loop photonic contributions significantly enhanced by the large logarithms [18].

The primary purpose of this work is to offer a theoretical background for the running and planned $\mu - e$ conversion experiments. We consider all the possible tree level contributions to $\mu - e$ conversion in the framework of the minimal SUSY model with most general form of R -parity violation (\tilde{R}_p MSSM) including the trilinear \tilde{R}_p couplings and the bilinear \tilde{R}_p lepton-Higgs terms. We also examine some non-SUSY and R_p SUSY mechanisms previously studied in [15, 16, 20]. We develop a formalism of calculating the $\mu - e$ conversion rate for the quark level Lagrangian with all these terms.

In our study we pay special attention to the effect of nucleon and nuclear structure dependence of the $\mu - e$ conversion branching ratio $R_{\mu e^-}$. In particular, we take into account the contribution of the strange nucleon sea which, as we will see, gives a contribution comparable to the contribution of the valence quarks of a nucleon.

Thus, we apply our formalism to the case of nuclei ^{48}Ti and ^{208}Pb by calculating numerically the muon-nucleus overlap integral and solving the Dirac equations with modern neural networks techniques and using the PSI experimental data. A similar application is done for the ^{27}Al target by employing the sensitivity of the designed MECO experiment.

Our final goal is to derive on this theoretical basis the experimental constraints on the \tilde{R}_p Yukawa couplings, the lepton-Higgs mixing parameters and on the sneutrino VEVs. Towards this end we use the experimental upper limits on the branching ratio $R_{\mu e^-}$ given above and derive the new stringent constraints on the R -parity violating parameters.

2 The effective $\mu - e$ conversion Lagrangian

It is well known that, the lepton flavors (L_i) and the total baryon (B) number are conserved by the standard model interactions in all orders of perturbation theory. As mentioned above, this is an accidental consequence of the SM field content and gauge invariance. Thus $\mu - e$ conversion is forbidden in the SM. In contrast to L_i the individual quark flavors B_i are not conserved in the SM by the charged current interactions due to the presence of non-trivial Cabibbo-Kobayashi-Maskawa (CKM) mixing matrix. L_i are conserved since the analogous mixing matrix can be rotated away by the neutrino fields redefinition. The latter is possible while the neutrino fields have no mass term and, therefore, are defined up to an arbitrary unitary rotation. As soon as the model is extended by inclusion of the right-handed neutrinos lepton flavor violation can occur since neutrinos may acquire a non-trivial mass matrix.

In the supersymmetric extensions of SM L_i and B conservation laws are in general violated. As a result potentially dangerous total lepton (\mathbb{L}) and baryon (\mathbb{B}) number violating processes become open.

One may easily eliminate \mathbb{L} and \mathbb{B} interactions from a SUSY model by introducing a discrete symmetry known as R-parity. This is a multiplicative Z_2 symmetry defined as $R_p = (-1)^{3B+L+2S}$, where S is the spin quantum number. In this framework neutrinos are massless. However the flavor violation in the lepton sector can occur at the 1-loop level via the L_i -violation in the slepton sector. Thus, $\mu^- - e^-$ conversion is allowed in the SUSY models with R-parity conservation.

There is no as yet convincing theoretical motivation for R-symmetry of the low energy Lagrangian and, therefore, SUSY models with (R_p SUSY) and without (\mathbb{R}_p SUSY) R-parity conservation are "a priori" both plausible.

Despite the above mentioned problems with \mathbb{L} , \mathbb{B} interactions \mathbb{R}_p SUSY looks rather attractive, since it may offer a clue to the solution of some long standing problems of particle physics, such as neutrino mass problem. In the \mathbb{R}_p SUSY framework neutrinos acquire Majorana masses at the weak-scale via mixing with the gauginos and higgsinos as well as via \mathbb{L} loop effects [21]. Furthermore, \mathbb{R}_p SUSY models admit non-trivial contributions to the lepton flavor violating processes. During the last few years the \mathbb{R}_p SUSY models have been extensively studied in the literature (for a recent review see Refs. [22]).

We analyze possible mechanisms for process (1) existing at the tree level in the minimal \mathbb{R}_p SUSY model with a most general form of R-parity violation.

A most general gauge invariant form of the R-parity violating part of the superpotential at the level of renormalizable operators reads

$$W_{\mathbb{R}_p} = \lambda_{ijk} L_i L_j E_k^c + \bar{\lambda}'_{ijk} L_i Q_j D_k^c + \mu_j L_j H_2 + \bar{\lambda}''_{ijk} U_i^c D_j^c D_k^c, \quad (6)$$

where L , Q stand for lepton and quark doublet left-handed superfields while E^c , U^c , D^c for lepton and *up*, *down* quark singlet superfields; H_1 and H_2 are the Higgs doublet superfields with a weak hypercharge $Y = -1, +1$, respectively. Summation over the generations is implied. The coupling constants λ ($\bar{\lambda}''$) are antisymmetric in the first (last) two indices. The bar sign in $\bar{\lambda}'$, $\bar{\lambda}''$ denotes that all the definitions are given in the gauge basis for the quark fields. Later on we will change to the mass basis and drop the bars. Henceforth we set $\bar{\lambda}'' = 0$ which are irrelevant for our consideration. This condition ensures the proton stability and can be guaranteed by special discrete symmetries other than R-parity.

The R-parity non-conservation brings into the SUSY phenomenology the lepton number (\mathbb{L}) and lepton flavor (\mathbb{L}_i) violation originating from the two different sources. One is given by the \mathbb{L} trilinear couplings in the superpotential $W_{\mathcal{R}_p}$ of Eq. (6). Another is related to the bilinear terms in $W_{\mathcal{R}_p}$ and in soft SUSY breaking sector. Presence of these bilinear terms leads to the terms linear in the sneutrino fields $\tilde{\nu}_i$ in the scalar potential. The linear terms drive these fields to non-zero vacuum expectation values $\langle \tilde{\nu}_i \rangle \neq 0$ at the minimum of the scalar potential. At this ground state the MSSM vertices $\tilde{Z}\nu\tilde{\nu}$ and $\tilde{W}e\tilde{\nu}$ produce the gaugino-lepton mixing mass terms $\tilde{Z}\nu\langle\tilde{\nu}\rangle, \tilde{W}e\langle\tilde{\nu}\rangle$ (with \tilde{W}, \tilde{Z} being wino and zino fields). These terms taken along with the lepton-higgsino $\mu_i L_i \tilde{H}_1$ mixing from the superpotential of Eq. (6) form 7×7 neutral fermion and 5×5 charged fermion mass matrices. For the considered case of $\mu - e$ conversion the only charged fermion mixing is essential. The charged fermion mass term takes the form

$$\mathcal{L}_{mass}^{(\pm)} = -\Psi_{(-)}'^T \mathcal{M}_{\pm} \Psi'_{(+)} - \text{H.c.} \quad (7)$$

in the basis of two component Weyl spinors corresponding to the weak eigenstate fields

$$\Psi_{(-)}'^T = (e_{-L}^-, \mu_{-L}^-, \tau_{-L}^-, -i\lambda_-, \tilde{H}_1^-), \quad \Psi_{(+)}'^T = (e_{+L}^+, \mu_{+L}^+, \tau_{+L}^+, -i\lambda_+, \tilde{H}_2^+). \quad (8)$$

Here λ_{\pm} are the SU_{2L} gauginos while the higgsinos are denoted as $\tilde{H}_{1,2}^{\pm}$. These fields are related to the mass eigenstate fields $\Psi_{(\pm)}$ by the rotation

$$\Psi_{(\pm)i} = \Delta_{ij}^{\pm} \Psi'_{(\pm)j}, \quad (9)$$

The unitary mixing matrices Δ^{\pm} diagonalize the chargino-charged lepton mass matrix as

$$(\Delta^-)^* \mathcal{M}_{\pm} (\Delta^+)^{\dagger} = \text{Diag}\{m_i^{(l)}, m_{\chi_k^{\pm}}\}, \quad (10)$$

where $m_i^{(l)}$ and $m_{\chi_k^{\pm}}$ are the physical charged lepton and chargino masses. In the present paper we use the notations of Refs. [23, 24].

Rotating the MSSM Lagrangian to the mass eigenstate basis according to Eq. (9) one obtains the new lepton number and lepton flavor violating interactions in addition to those which are present in the superpotential Eq. (6). Note that the mixing between the charged leptons (e_{+L}^+, μ_{+L}^+) and the chargino components $(-i\lambda_+, \tilde{H}_2^+)$, described by the off diagonal blocks of the Δ^+ , is proportional to the small factor $\sim m_{e,\mu}/M_{SUSY}$ [23, 24] and is, therefore, neglected in our analysis.

Let us write down the MSSM terms generating by the rotation (9) the new lepton flavor violating interactions relevant for the $\mu^- - e^-$ conversion. In the two component form they can be written as [25]

$$\mathcal{L}_{MSSM} = \frac{g_2}{2 \cos \theta_W} Z^{\mu} \bar{\Psi}'_i A_{ij} \bar{\sigma}_{\mu} \Psi'_j + i g_2 \lambda^- u_L \tilde{d}_L^*, \quad (11)$$

where $A_{ij} = (1 - 2 \sin^2 \theta_W) \delta_{ij} + \delta_{i4} \delta_{4j}$. Rotating this equation to the mass eigenstate basis we write down in the four-component Dirac notation

$$\mathcal{L}_{MSSM} = \frac{g_2}{2 \cos \theta_W} a_Z Z^{\mu} \bar{e} \gamma_{\mu} P_L \mu + g_2 \zeta_i \cdot \bar{u}_k P_R e_i^c \tilde{d}_{Lk}. \quad (12)$$

Here $e_i = (e, \mu, \tau)$, $P_{L,R} = (1 \mp \gamma_5)/2$. The lepton flavor violating parameters in this formula are given by

$$a_Z = \Delta_{14}^- \Delta_{24}^{-*} \approx \xi_{11} \xi_{21}^*, \quad \zeta_i = \Delta_{i4}^{-*} \approx \xi_{i1}. \quad (13)$$

The approximate expressions for these parameters were found by the method of Ref. [23] expanding the mixing matrix Δ^- in the small matrix parameter

$$\xi_{i1}^* = \frac{g_2(\mu \langle \tilde{\nu}_i \rangle - \langle H_1 \rangle \mu_i)}{\sqrt{2} (M_2 \mu - \sin 2\beta M_W^2)}, \quad (14)$$

where μ, M_2 are the ordinary MSSM mass parameters from the superpotential term $\mu H_1 H_2$ and from the SU_2 gaugino soft mass term $M_2 \tilde{W}^k \tilde{W}^k$. The MSSM mixing angle is defined as $\tan \beta = \langle H_2 \rangle / \langle H_1 \rangle$. The other lepton flavor violating interaction contributing to the $\mu^- - e^-$ conversion come from the superpotential (6).

The leading diagrams describing possible tree level \mathcal{R}_p MSSM contributions to the $\mu - e$ conversion are presented in Fig. 1. The vertex operators encountered in these diagrams are

$$\begin{aligned} \mathcal{L}_{\mu e^-} = & 2 \lambda_{i21} \tilde{\nu}_{Li} \bar{e} P_L \mu + \lambda'_{ijj} \tilde{\nu}_{Li} \bar{d}_j P_L d_j - \lambda'^*_{ijk} V_{nj} \left(\tilde{u}_{Ln}^* \bar{e}_i P_R d_k + \tilde{d}_{Rk} \bar{u}_n P_R e_i^c \right) + \\ & + g_2 \zeta_i V_{nk} \cdot \bar{u}_n P_R e_i^c \tilde{d}_{Lk} + \frac{1}{2} \frac{g_2}{\cos \theta_W} a_Z Z^\mu \bar{e} \gamma_\mu P_L \mu - \frac{g_2}{\cos \theta_W} Z^\mu \bar{q} \gamma_\mu (\epsilon_L P_L + \epsilon_R P_R) q, \end{aligned} \quad (15)$$

where the first three terms originate from the superpotential (6), the fourth and fifth terms correspond to the chargino-charged lepton mixing terms in Eq. (12) and the last one is the ordinary SM neutral current interaction.

In Eq. (15) the SM neutral current parameters are defined as usual

$$\epsilon_L = T_3 - \sin^2 \theta_W Q, \quad \epsilon_R = -\sin^2 \theta_W Q$$

with T_3 and Q being the 3rd component of the weak isospin and the electric charge.

The Lagrangian (15) is given in the quark mass eigenstate basis which is related to the flavor basis q^0 through

$$q_{L,R} = V_{L,R}^q \cdot q^0.$$

For convenience we introduced the new couplings

$$\lambda'_{ijk} = \bar{\lambda}'_{imn} \left(V_L^d \right)_{jm}^* \left(V_R^d \right)_{kn}.$$

The CKM matrix is defined in the standard way as $V = V_L^u V_L^{d\dagger}$.

Integrating out the heavy fields from the diagrams in Fig. 1 and carrying out Fierz reshuffling we obtain the 4-fermion effective Lagrangian which describes the $\mu - e$ conversion at the quark level in the first order of perturbation theory. It takes the form

$$\mathcal{L}_{eff}^q = \frac{G_F}{\sqrt{2}} j_\mu \left[\eta_L^{ui} J_{uL(i)}^\mu + \eta_R^{ui} J_{uR(i)}^\mu + \eta_L^{di} J_{dL(i)}^\mu + \eta_R^{di} J_{dR(i)}^\mu \right] + \frac{G_F}{\sqrt{2}} \left[\bar{\eta}_R^{di} J_{dR(i)} j_L + \bar{\eta}_L^{di} J_{dL(i)} j_R \right]. \quad (16)$$

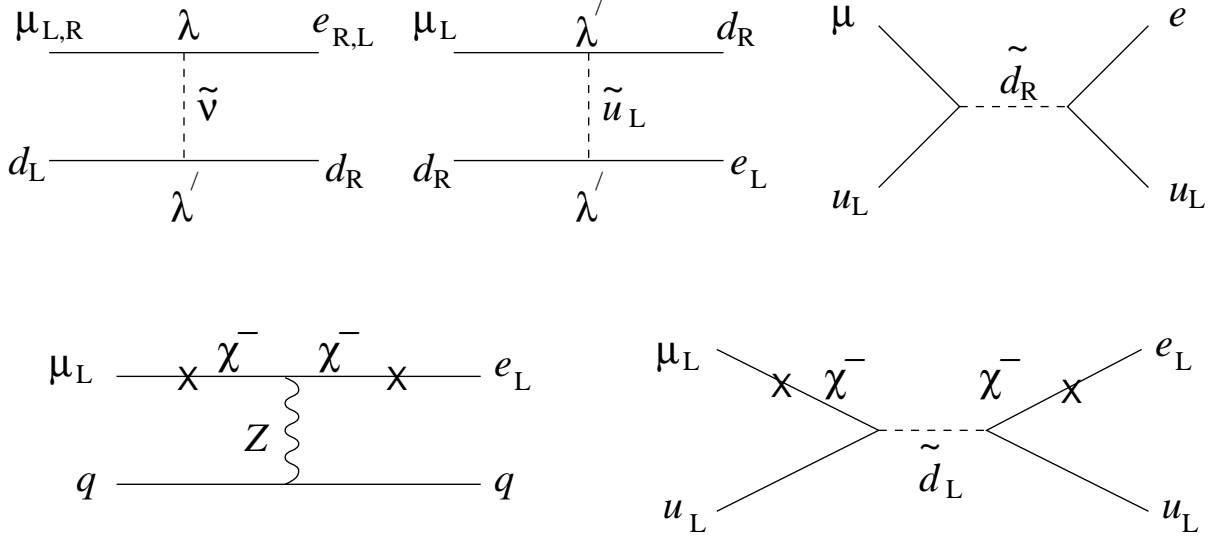


Figure 1: Leading \mathcal{R}_p MSSM diagrams contributing to $\mu - e$ conversion at the tree level. (i) The upper diagrams originate from the trilinear λ, λ' terms in the superpotential Eq. (6). (ii) The lower diagrams originate from the chargino-charged lepton mixing schematically denoted by crosses (X) on the lepton lines.

The index i denotes generation so that $u_i = u, c, t$ and $d_i = d, s, b$. The coefficients η accumulate dependence on the \mathcal{R}_p SUSY parameters in the form

$$\begin{aligned}
\eta_L^{ui} &= -\frac{1}{\sqrt{2}} \sum_{l,m,n} \frac{\lambda'_{2ln} \lambda_{1mn}^*}{G_F \tilde{m}_{dR(n)}^2} V_{il}^* V_{im} + 2(1 - \frac{4}{3} \sin^2 \theta_W) a_Z + 4 \sum_n \zeta_1 \zeta_2^* \frac{M_W^2}{\tilde{m}_{dL(n)}^2} |V_{in}|^2, \\
\eta_R^{di} &= \frac{1}{\sqrt{2}} \sum_{l,m,n} \frac{\lambda'_{2mi} \lambda_{1li}^*}{G_F \tilde{m}_{uL(n)}^2} V_{nm}^* V_{nl} + \frac{4}{3} \sin^2 \theta_W a_Z, \\
\eta_L^{di} &= -2(1 - \frac{2}{3} \sin^2 \theta_W) a_Z, \quad \eta_R^{ui} = -\frac{8}{3} \sin^2 \theta_W a_Z \\
\bar{\eta}_L^{di} &= -\sqrt{2} \sum_n \frac{\lambda'_{nii} \lambda_{n12}^*}{G_F \tilde{m}_{\nu(n)}^2}, \quad \bar{\eta}_R^{di} = -\sqrt{2} \sum_n \frac{\lambda_{nii}^* \lambda_{n21}}{G_F \tilde{m}_{\nu(n)}^2}.
\end{aligned} \tag{17}$$

Here $\tilde{m}_{q(n)}, \tilde{m}_{\nu(n)}$ are the squark and sneutrino masses. In Eq. (16) we introduced the color singlet currents

$$J_{q_{L/R}(i)}^\mu = \bar{q}_i \gamma^\mu P_{L/R} q_i, \quad J_{d_{L/R}(i)} = \bar{d}_i P_{L/R} d_i, \quad j^\mu = \bar{e} \gamma^\mu \mu, \quad j_{L/R} = \bar{e} P_{L/R} \mu, \tag{18}$$

where $q_i = (u_i, d_i)$.

Since in the next sections we report the new results for the nuclear matrix elements of ^{48}Ti , ^{27}Al and ^{208}Pb we are going also to update $\mu^- \rightarrow e^-$ constraints on the effective lepton flavor violating parameters corresponding to certain non-SUSY and R_p SUSY mechanisms

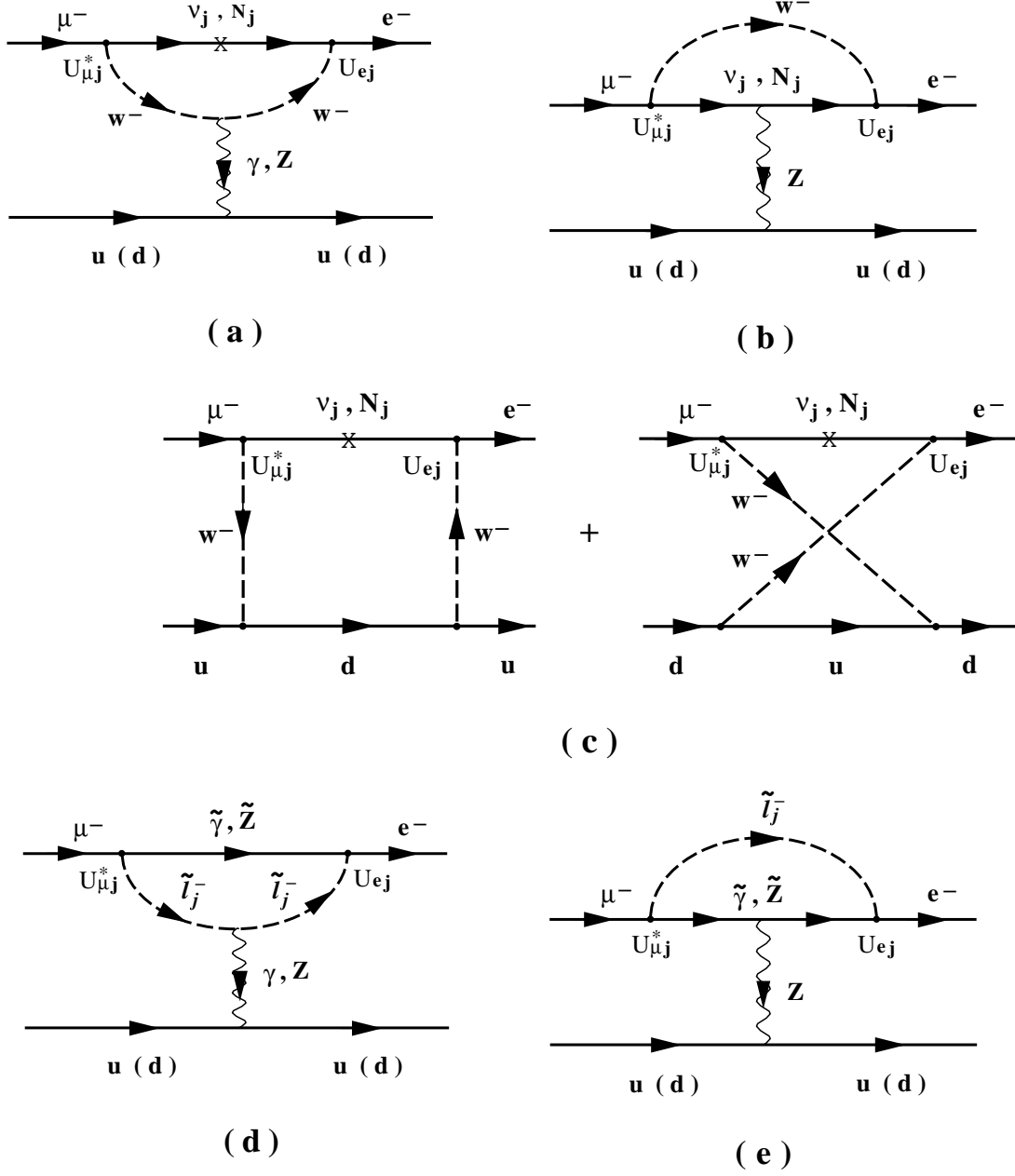


Figure 2: Photonic and non-photonic mechanisms of the $\mu^- - e^-$ conversion within some extensions of the standard model: (a-c) the SM with massive neutrinos and (a-c) R-parity conserving supersymmetric extensions of the SM.

shown in Fig. 2. These mechanisms were previously studied in Refs. [16, 20]. Let us shortly summarize these mechanisms for completeness. The long-distance photonic mechanisms mediated by the photon exchange between the quark and the $\mu - e$ -lepton currents is realized at the 1-loop level as the $\nu - W$ loop [Fig. 2(a)] with the massive neutrinos ν_i and the loop with the supersymmetric particles such as the neutralino(chargino)-slepton(sneutrino) [Fig. 2(d)]. In the R-parity violating SUSY models there are also lepton-slepton and quark-squark loops generated by the superpotential couplings λLLE^c and $\lambda' LQD^c$ respectively [18]. The

short-distance non-photonic mechanisms in Fig. 2 contain heavy particles in intermediate states and is realized at the 1-loop level [Fig. 2(a,b,d,e)] or at the level of box diagrams [Fig. 2(c)]. The 1-loop diagrams of the non-photonic mechanisms include the diagrams similar to those for the photonic mechanisms but with the Z-boson instead of the photon [Fig. 2(a,d)] as well as additional Z-boson couplings to the neutrinos and neutralinos [Fig. 2(b,e)]. The box diagrams are constructed of the W-bosons and massive neutrinos [Fig. 2(c)] as well as similar boxes with neutralinos and sleptons or charginos and sneutrinos. The branching ratio formula for these mechanisms is given in the next section.

3 Nucleon and nuclear Structure dependence of the $\mu - e$ conversion rates.

One of the main goals of this paper is the calculation of the $\mu - e$ conversion rate using realistic form factors of the participating nucleus (A,Z). This can be achieved by applying the conventional approach based on the well known non-relativistic impulse approximation, i.e. treating the nucleus as a system of free nucleons [4]. To follow this approach as a first step one has to reformulate the $\mu - e$ conversion effective Lagrangian (16) specified at the quark level in terms of the nucleon degrees of freedom.

The transformation of the quark level effective Lagrangian, \mathcal{L}_{eff}^q , to the effective Lagrangian at the nucleon level, \mathcal{L}_{eff}^N , is usually done by utilizing the on-mass-shell matching condition [26]

$$\langle \Psi_F | \mathcal{L}_{eff}^q | \Psi_I \rangle \approx \langle \Psi_F | \mathcal{L}_{eff}^N | \Psi_I \rangle, \quad (19)$$

where $|\Psi_I\rangle$ and $\langle \Psi_F|$ are the initial and final nucleon states. In order to solve this equation we use various relations for the matrix elements of the quark operators between the nucleon states

$$\langle N | \bar{q} \Gamma_K q | N \rangle = G_K^{(q,N)} \bar{\Psi}_N \Gamma_K \Psi_N, \quad (20)$$

with $q = \{u, d, s\}$, $N = \{p, n\}$ and $K = \{V, A, S, P\}$, $\Gamma_K = \{\gamma_\mu, \gamma_\mu \gamma_5, 1, \gamma_5\}$. Since the maximum momentum transfer \mathbf{q}^2 in $\mu - e$ conversion, i.e. $|\mathbf{q}| \approx m_\mu/c$ with $m_\mu = 105.6 MeV$ the muon mass, is much smaller than the typical scale of nucleon structure we can safely neglect the \mathbf{q}^2 -dependence of the nucleon form factors $G_K^{(q,N)}$. For the same reason we drop the weak magnetism and the induced pseudoscalar terms proportional to the small momentum transfer.

The isospin symmetry requires that

$$G_K^{(u,n)} = G_K^{(d,p)} \equiv G_K^d, \quad G_K^{(d,n)} = G_K^{(u,p)} \equiv G_K^u, \quad G_K^{(s,n)} = G_K^{(s,p)} \equiv G_K^s, \quad (21)$$

with $K = V, A, S, P$. Conservation of vector current postulates the vector charge to be equal to the quark number of the nucleon. This allows fixing of the vector nucleon constants

$$G_V^u = 2, \quad G_V^d = 1, \quad G_V^s = 0. \quad (22)$$

The axial-vector form factors G_A can be extracted from the experimental data on polarized nucleon structure functions [27, 28] combined with the data on hyperon semileptonic decays

[29]. The result is

$$G_A^u \approx 0.78, \quad G_A^d \approx -0.47, \quad G_A^s \approx -0.19. \quad (23)$$

The scalar form factors are extracted from the baryon octet B mass spectrum M_B in combination with the data on the pion-nucleon sigma term

$$\sigma_{\pi N} = (1/2)(m_u + m_d)\langle p|\bar{u}u + \bar{d}d|p\rangle. \quad (24)$$

Towards this end we follow the QCD picture of the baryon masses which is based on the relation [30, 31]

$$\langle B|\theta_\mu^\mu|B\rangle = M_B \bar{B}B \quad (25)$$

and on the well known representation for the trace of the energy-momentum tensor [30]

$$\theta_\mu^\mu = m_u \bar{u}u + m_d \bar{d}d + m_s \bar{s}s - (\tilde{b}\alpha_s/8\pi)G_{\mu\nu}^a G_a^{\mu\nu}, \quad (26)$$

where $G_{\mu\nu}^a$ is the gluon field strength, α_s is the QCD coupling constant and \tilde{b} is the reduced Gell-Mann-Low function with the heavy quark contribution subtracted. Using these relations in combination with $SU(3)$ relations [31] for the matrix elements $\langle B|\theta_\mu^\mu|B\rangle$ as well as the experimental data on M_B and $\sigma_{\pi N}$ we derive

$$G_S^u \approx 5.1, \quad G_S^d \approx 4.3, \quad G_S^s \approx 2.5. \quad (27)$$

The nucleon matrix elements of the pseudoscalar quark currents can be related to the divergence of the baryon octet axial vector currents [31]. Utilizing this fact we find the pseudoscalar form factors

$$G_P^u \approx 103, \quad G_P^d \approx 100, \quad G_P^s \approx 3.3. \quad (28)$$

Note that the strange quarks of the nucleon sea significantly contribute to the nucleon form factors G_A , G_P and G_S . This result dramatically differs from the naïve quark model and the MIT bag model where $G_{A,S,P}^s = 0$. The contribution of the strange nucleon sea will allow us to extract additional constraints on the second generation \mathcal{R}_p parameters.

Now we can solve Eq. (19) and write the effective $\mu - e$ conversion Lagrangian at the nucleon level as

$$\mathcal{L}_{eff}^N = \frac{G_F}{\sqrt{2}} \left[\bar{e}\gamma_\mu(1 - \gamma_5)\mu \cdot J^\mu + \bar{e}\mu \cdot J^+ + \bar{e}\gamma_5\mu \cdot J^- \right]. \quad (29)$$

where we have introduced the nucleon currents

$$\begin{aligned} J^\mu &= \bar{N}\gamma^\mu \left[(\alpha_V^{(0)} + \alpha_V^{(3)}\tau_3) + (\alpha_A^{(0)} + \alpha_A^{(3)}\tau_3)\gamma_5 \right] N, \\ J^\pm &= \bar{N} \left[(\alpha_{\pm S}^{(0)} + \alpha_{\pm S}^{(3)}\tau_3) + (\alpha_{\pm P}^{(0)} + \alpha_{\pm P}^{(3)}\tau_3)\gamma_5 \right] N, \end{aligned} \quad (30)$$

for nucleon isospin doublet $N^T = (p, n)$. The coefficients in Eq. (30) are defined as

$$\begin{aligned}
\alpha_V^{(0)} &= \frac{1}{8}(G_V^u + G_V^d)(\eta_R^{u1} + \eta_L^{u1} + \eta_R^{d1} + \eta_L^{d1}), \\
\alpha_V^{(3)} &= \frac{1}{8}(G_V^u - G_V^d)(\eta_R^{u1} + \eta_L^{u1} - \eta_R^{d1} - \eta_L^{d1}), \\
\alpha_A^{(0)} &= \frac{1}{8}(G_A^u + G_A^d)(\eta_R^{u1} - \eta_L^{u1} + \eta_R^{d1} - \eta_L^{d1}) + \frac{1}{4}G_A^s(\eta_R^{d2} - \eta_L^{d2}), \\
\alpha_A^{(3)} &= \frac{1}{8}(G_A^u - G_A^d)(\eta_R^{u1} - \eta_L^{u1} - \eta_R^{d1} + \eta_L^{d1}), \\
\alpha_{\pm S}^{(0)} &= \frac{1}{16}(G_S^u + G_S^d)(\bar{\eta}_L^{d1} \pm \bar{\eta}_R^{d1}) + \frac{1}{8}G_S^s(\bar{\eta}_L^{d2} \pm \bar{\eta}_R^{d2}), \\
\alpha_{\pm S}^{(3)} &= -\frac{1}{16}(G_S^u - G_S^d)(\bar{\eta}_L^{d1} \pm \bar{\eta}_R^{d1}), \\
\alpha_{\pm P}^{(0)} &= -\frac{1}{16}(G_P^u + G_P^d)(\bar{\eta}_L^{d1} \mp \bar{\eta}_R^{d1}) - \frac{1}{8}G_P^s(\bar{\eta}_L^{d2} \mp \bar{\eta}_R^{d2}), \\
\alpha_{\pm P}^{(3)} &= \frac{1}{16}(G_P^u - G_P^d)(\bar{\eta}_L^{d1} \mp \bar{\eta}_R^{d1}),
\end{aligned} \tag{31}$$

Starting from the Lagrangian (29) it is straightforward to deduce the formula for the total $\mu - e$ conversion rate. In the present paper we focus on the coherent process, i.e. ground state to ground state transitions. This is a dominant channel of $\mu - e$ conversion which, in most of the experimentally interesting nuclei, exhausts more than 90% of the total $\mu^- \rightarrow e^-$ branching ratio [14, 15]. To the leading order of the non-relativistic expansion the coherent $\mu - e$ conversion rate takes the form

$$\Gamma_{\mu e^-}^{coh} = \frac{G_F^2 p_e E_e}{2\pi} \mathcal{Q}(\mathcal{M}_p + \mathcal{M}_n)^2, \tag{32}$$

where

$$\begin{aligned}
\mathcal{Q} &= 2|\alpha_V^{(0)} + \alpha_V^{(3)} \phi|^2 + |\alpha_{+S}^{(0)} + \alpha_{+S}^{(3)} \phi|^2 + |\alpha_{-S}^{(0)} + \alpha_{-S}^{(3)} \phi|^2 \\
&\quad + 2 \operatorname{Re}\{(\alpha_V^{(0)} + \alpha_V^{(3)} \phi)[\alpha_{+S}^{(0)} + \alpha_{-S}^{(0)} + (\alpha_{+S}^{(3)} + \alpha_{-S}^{(3)}) \phi]\}.
\end{aligned} \tag{33}$$

The transition matrix elements $\mathcal{M}_{p,n}$ in Eq. (32) depend on the final nuclear state populated during the $\mu - e$ conversion. We should stress that, after computing the nuclear matrix elements $\mathcal{M}_{p,n}$ the data provide constraints on the quantity \mathcal{Q} of Eq. (33). For the ground state to ground state transitions in spherically symmetric nuclei the following integral representation is valid

$$\mathcal{M}_{p,n} = 4\pi \int j_0(p_e r) \Phi_\mu(r) \rho_{p,n}(r) r^2 dr \tag{34}$$

where $j_0(x)$ the zero order spherical Bessel function and $\rho_{p,n}$ the proton (p), neutron (n) nuclear density normalized to the atomic number Z and neutron number N of the participating nucleus, respectively. The space dependent part of the muon wave function Φ_μ is a spherically symmetric function which in our calculations (see Sect. 4) was obtained by solving numerically the Shrödinger and Dirac equations with the Coulomb potential.

In defining \mathcal{Q} , Eq. (33), we introduced the ratio

$$\phi = (\mathcal{M}_p - \mathcal{M}_n)/(\mathcal{M}_p + \mathcal{M}_n) \approx (A - 2Z)/A, \quad (35)$$

where A and Z are the atomic weight and the total charge of the nucleus. The quantity \mathcal{Q} depends weakly on the nuclear parameters through the factor ϕ . In fact, the terms depending on ϕ are small since $\phi < 1$ (see Table 1) and G_S^u, G_S^d as well as G_V^u, G_V^d have the same sign. In practice the nuclear dependence of \mathcal{Q} can be neglected and thus, \mathcal{Q} coincides with the value of 2ρ where ρ is defined below. It can be considered as a universal effective \mathcal{R}_p parameter measuring the \mathcal{R}_p SUSY contribution to the $\mu - e$ conversion. It also represents a suitable characteristic which allows comparison of $\mu - e$ conversion experiments on different targets treating the corresponding upper bounds on \mathcal{Q} as their sensitivities to the \mathcal{R}_p SUSY signal.

For completeness, in Sect. 4 the limits for some non-SUSY [16, 20] as well as \mathcal{R}_p SUSY contributions to the $\mu^- - e^-$ nuclear conversion (see in Fig. 2) are updated. The corresponding expression for $R_{\mu e^-}$ is written as [13]

$$R_{\mu e^-} = \rho \gamma, \quad (36)$$

where ρ is nearly independent of nuclear physics [15] and contains the lepton flavor violating parameters corresponding to the contributions in Fig. 2. Thus, e.g. for photon-exchange mode ρ is given by

$$\rho = (4\pi\alpha)^2 \frac{|f_{M1} + f_{E0}|^2 + |f_{E1} + f_{M0}|^2}{(G_F m_\mu^2)^2} \quad (37)$$

where the four electromagnetic form factors $f_{E0}, f_{E1}, f_{M0}, f_{M1}$ are parametrized in a specific elementary model [15].

The factor $\gamma(A, Z)$ in Eq. (36) accumulates about all the nuclear structure dependence of the branching ratio $R_{\mu e^-}$. Assuming that the total rate of the ordinary muon capture is given by the Goulard-Primakoff function, f_{GP} , the nuclear structure factor $\gamma(A, Z)$ takes the form

$$\gamma(A, Z) \equiv \gamma = \frac{E_e p_e}{m_\mu^2} \frac{M^2}{G^2 Z f_{GP}(A, Z)}, \quad (38)$$

where $G^2 \approx 6$. Thus, a non-trivial nuclear structure dependence of the $\mu^- \rightarrow e^-$ conversion branching ratio $R_{\mu e^-}$ is mainly concentrated in the nuclear matrix elements M^2 [5]. In the proton-neutron representation one can write down

$$M^2 = [M_p + Q M_n]^2 \quad (39)$$

where Q takes the values of Eq. (32) of Ref. [15a] and $M_{p,n}$ are given by writing the matrix elements of Eq. (34) in terms of an effective muon wavefunction as

$$\mathcal{M}_{p,n} = \langle \Phi_\mu \rangle M_{p,n} \quad (40)$$

In our present approach the role of ρ in Eq. (36) is played by \mathcal{Q} , since $\mathcal{Q} = 2\rho$, and the corresponding γ function defined in Eq. (38) for R-parity violating interactions, $\gamma_{\mathcal{R}_p}$, is obtained from Eq. (38) by putting $Q = 1$ in Eq. (39). The separation of nuclear physics from the elementary particle parameters is not complete but we have seen that ϕ is quite small. In any case we present in Table 1 the values of ϕ for the various nuclear systems.

4 Results and Discussion.

The pure nuclear physics calculations needed for the $\mu - e$ conversion studies refer to the integrals of Eq. (34). The results of \mathcal{M}_p and \mathcal{M}_n for the currently interesting nuclei Al , Ti and Pb are shown in Table 2. They have been calculated using proton densities ρ_p from the electron scattering data [32] and neutron densities ρ_n from the analysis of pionic atom data [33]. We employed an analytic form for the muon wave function $\Phi_\mu(r)$ obtained by solving the Schrödinger equation using the Coulomb potential produced by the charge densities discussed above. This way the finite size of a nucleus was taken into consideration. Moreover, we included vacuum polarization corrections as in Ref. [14]. In solving the Schrödinger equation we have used modern neural networks techniques [34] which give the wave function $\Phi_\mu(r)$ in the analytic form of a sum over sigmoid functions. Thus, in Eq. (34) only a simple numerical integration is finally required. To estimate the influence of the non-relativistic approximation on the muon wave function $\Phi_\mu(\mathbf{r})$, we have also determined it by solving the Dirac equation. The results for $\mathcal{M}_{p,n}$ do not significantly differ from those of the Schrödinger picture. In Table 2 we also show the muon binding energy ϵ_b (obtained as output of the Dirac and Schrödinger solution) and the experimental values for the total rate of the ordinary muon capture $\Gamma_{\mu c}$ taken from Ref. [35].

Using the values of \mathcal{M}_p , \mathcal{M}_n for a set of nuclei throughout the periodic table we can estimate the nuclear structure dependence of the $\mu - e$ conversion branching ratio, i.e. the function $\gamma(A, Z)$ in Eq. (36). The results are quoted in Table 3. For comparison in this table we also list the results of $\gamma_{\mathcal{R}_p}$ corresponding to the \mathcal{R}_p SUSY mechanisms studied in the present paper and calculated as we stated in Sect. 3. These results can be exploited for setting constraints on the quantities ρ and \mathcal{Q} corresponding to specific models predicting the $\mu - e$ process.

In Table 4 we quote the upper bounds for the quantities ρ and \mathcal{Q} corresponding to the mechanisms shown in Figs. 1,2. These bounds were derived from the recent experimental upper bounds on the branching ratio $R_{\mu e^-}$ for Ti and Pb targets given in (3) and (4) and from the expected experimental sensitivity (5) of the Brookhaven MECO experiment. The limits on ρ and \mathcal{Q} quoted in Table 4 for ^{27}Al are improvements by about four orders of magnitude over the existing ones.

We should stress that limits on the quantities ρ of Eq. (37) and \mathcal{Q} of Eq. (33), are the only constraints imposed by the $\mu - e$ conversion on the underlying elementary particle physics. One can extract upper limits on the individual lepton flavor violation parameters (\mathcal{R}_p couplings, effective scalar and vector couplings, neutrino masses etc. [1, 5, 15, 19]) under certain assumptions like the commonly assumed dominance of only one component of the $\mu - e$ conversion Lagrangian which is equivalent to constrain one parameter or product of the parameters at a time. Using the upper limits for \mathcal{Q} given in Table 3 we can derive under the above assumptions the constraints on $\alpha_K^{(\tau)}$ of Eq. (33) and the products of various \mathcal{R}_p parameters. Thus, the bounds obtained for the scalar current couplings $\alpha_{\pm S}^{(0)}$ in the R -parity violating Lagrangian for the ^{27}Al target [8] are $|\alpha_{\pm S}^{(0)}| < 7 \times 10^{-10}$. The limit for $\alpha_{\pm S}^{(0)}$ obtained with the data for the Ti target [9] is $|\alpha_{\pm S}^{(0)}| < 1.1 \times 10^{-7}$, i.e. more than two orders of magnitude weaker than the limit of ^{27}Al .

With these limits it is straightforward to derive constraints on the parameters of the

initial Lagrangian (15). In Tables 5,6 we list the upper bounds on the products of the trilinear \mathcal{R}_p couplings which we obtained from the experimental limit on $\mu - e$ conversion in ^{48}Ti and from the expected experimental sensitivity of MECO detector using ^{27}Al as a target material. The corresponding constraints for ^{208}Pb are significantly weaker and not presented here. In Tables 5,6 the quantity B denotes a scaling factor defined as

$$B_{Ti} = (R_{\mu e}^{exp}/6.1 \times 10^{-13})^{1/2}, \quad B_{Al} = (R_{\mu e}^{exp}/2.0 \times 10^{-17})^{1/2}, \quad (41)$$

which can be used for reconstructing the limits on the listed products of the \mathcal{R}_p parameters corresponding to the other experimental upper limits on the branching ratio $R_{\mu e}^{exp}$. In the 2nd column of Tables 5,6 we present previous limits existing in the literature and taken from [18, 22]. As seen from Tables 5,6 the $\mu - e$ -conversion limits on the products $\lambda'\lambda'$ and $\lambda\lambda'$, except only $\lambda'_{232}\lambda'_{132}$ and $\lambda'_{233}\lambda'_{133}$, are significantly more stringent than those previously known in the literature. The two products $\lambda'\lambda'$ and $\lambda\lambda'$ are less stringently constrained by the present experimental data on ^{48}Ti within the tree level non-photonic mechanism. Note that the corresponding previous constraints on these products (2nd column of Table 5) were obtained from the photonic 1-loop mechanism [18] of $\mu^- - e^-$ conversion which are better than existing in the literature non- $\mu^- \rightarrow e^-$ constraints on $\lambda'\lambda'$ and $\lambda\lambda'$. The products in Table 6 are not constrained by this mechanism [18]. However it constrains the products $\lambda\lambda$ not constrained by the tree level \mathcal{R}_p SUSY mechanism. At present the $\mu^- \rightarrow e^-$ constraints on $\lambda\lambda$ within the 1-loop \mathcal{R}_p SUSY mechanism are weaker than those derived from the other processes. As we have mentioned at the beginning, significant improvement on these $\mu^- \rightarrow e^-$ limits is expected from the ongoing experiments at PSI [9] and even better from the MECO experiment at Brookhaven [6]. This would make the $\mu - e$ conversion constraints on all the products of the \mathcal{R}_p trilinear coupling attainable in the $\mu - e$ conversion at the tree and at the 1-loop levels better than those from the other processes in all the cases.

Note that the last four limits for $\lambda'\lambda$ in Table 6 originate from the contribution of the strange nucleon sea. These limits are comparable to the other $\mu^- \rightarrow e^-$ constraints derived from the valence quarks contributions.

Finally we put constraints on the products of the bilinear \mathcal{R}_p parameters evaluated from the $\mu - e$ conversion in ^{48}Ti as

$$\langle \tilde{\nu}_1 \rangle \langle \tilde{\nu}_2 \rangle, \mu_1 \mu_2, \langle \tilde{\nu}_1 \rangle \mu_2, \langle \tilde{\nu}_2 \rangle \mu_1 \leq (80\text{MeV})^2 \left(\frac{\tilde{m}}{100\text{GeV}} \right)^2 B, \quad (42)$$

where B is a scaling factor defined in Eq. (41). These constraints are weaker than those derived in Ref. [36] from the Super-Kamiokande atmospheric neutrino data.

The limits in Tables 5,6 and in Eq. (42) were extracted under the following assumptions. We assumed that all the scalar masses in Eq. (17) are equal $\tilde{m}_{uL(n)} \approx \tilde{m}_{dL,R(n)} \approx \tilde{m}_{\nu(n)} \approx \tilde{m}$ and also that there is no significant compensation between the different terms contributing to the ratio $R_{\mu e^-}$. Note that the last assumption is, in practice, equivalent to the other well known assumptions about the dominance of only one parameter or product of the parameters at a time. These assumptions are widely used in the literature for derivation of constraints on the R-parity violating parameters.

Instead of considering only one specific combination of λ and λ' as dominant, one may attempt to consider all combinations of the R-parity violating couplings. To this end one

needs constraints on the relative magnitudes of the R-parity violating couplings. This can be accomplished in a fashion analogous to the theory of textures for the Yukawa couplings. This theory, which expresses the entries of the down fermion mass matrix in powers of a parameter $\bar{\epsilon} = 0.23$, has been successful in describing the charged fermion mass matrices (for review see [37] and references therein). This can be extended to the R-parity violation couplings themselves [38, 39]. In fact using solution B of Ref. [39] we obtain

$$\lambda'_{112} = \lambda'_{121} = \lambda'_{212} = \lambda', \quad \lambda_{121} = \bar{\epsilon}^2 \lambda' \quad (43)$$

This way, $\mu - e$ conversion can be used to constrain the overall scale of the R-parity violating interaction using phenomenologically acceptable textures [39].

5 Summary and Conclusions.

The transition matrix elements of the flavor violating $\mu^- - e^-$ conversion are of notable importance in computing accurately the corresponding rates for each accessible channel of this exotic process. Such calculations provide useful nuclear-physics inputs for the expected new data from the PSI and MECO experiments to put more severe bounds on the muon-number violating parameters determining the effective currents in various models that predict the exotic $\mu^- \rightarrow e^-$ process.

We developed a systematic approach which allows one to calculate the $\mu^- - e^-$ conversion rate in terms of the quark level Lagrangian of any elementary model taking into account the effect of the nucleon and nuclear structure. Our conversion rate formula (32) is valid for the interactions with the (axial-)vector and (pseudo-)scalar quark and lepton currents, as shown in Eq. (29). In the previous $\mu^- \rightarrow e^-$ calculations found in the literature only the (axial-)vector currents were considered.

In the case of the R-parity violating interactions discussed here we have investigated all the possible tree level contributions to the $\mu - e$ conversion in nuclei. We found new important contribution to $\mu^- - e^-$ conversion originating from the strange quark sea in the nucleon which is comparable with the usual contribution of the valence u, d quarks.

We introduced the quantities ρ and \mathcal{Q} defined in Eqs. (37) and (33) which can be associated with theoretical sensitivities of a $\mu^- - e^-$ conversion experiment to the charged lepton flavor violating interactions discussed in the present paper. These quantities are independent of a target material and, therefore, might be helpful for comparison of searching potentials of different $\mu - e$ conversion experiments and for planning future experiments.

From the existing data on $R_{\mu e^-}$ in ^{48}Ti and ^{208}Pb and the expected sensitivity of the designed MECO experiment [6] we obtained stringent upper limits on the quantities ρ and \mathcal{Q} . Then we extracted the limits on the products of the trilinear \mathcal{R}_p parameters of the type $\lambda\lambda', \lambda'\lambda'$ which are significantly more severe than those existing in the literature.

Let us conclude with the following important remark. As was observed in Refs. [18, 19], if the ongoing experiments at PSI [10] and Brookhaven [6] will have reached the quoted sensitivities in the branching ratio $R_{\mu e^-}$ then the $\mu^- \rightarrow e^-$ constraints on all the products of the \mathcal{R}_p parameters $\lambda\lambda, \lambda'\lambda, \lambda'\lambda'$ measurable in $\mu - e$ conversion will become more stringent than those from any other processes. This is especially important since no comparable

improvements of the other experiments probing these couplings is expected in the near future.

Acknowledgments

The research described in this publication was made possible in part by the INTAS grant 93-1648-EXT and Fondecyt (Chile) under grant 1000717. JDV would like to express his appreciation to the Humboldt Foundation for their award and thanks to the Institute of Theoretical Physics at University of Tübingen for hospitality. S.K. thanks V.A. Bednyakov and F. Simkovic for discussions.

References

- [1] W.J. Marciano and A.I. Sanda, Phys. Rev. Lett. **38** (1977) 1512; W.J. Marciano and A.I. Sanda, Phys. Lett. **B 67** (1977) 303.
- [2] T.P. Cheng and L.F. Li, Phys. Rev. **D 16** (1977) 1425; O. Shanker, Phys. Rev **D 20** (1979) 1608.
- [3] J.D. Vergados, Phys. Reports **133** (1986) 1.
- [4] J. Bernabeau, E. Nardi and D. Tomasini, Nucl. Phys. **B 409** (1993) 69.
- [5] T.S. Kosmas, G.K. Leontaris and J.D. Vergados, Prog. Part. Nucl. Phys. **33** (1994) 397.
- [6] W. Molzon, The MECO Experiment: A search for $\mu^- N \rightarrow e^- N$ with sensitivity below 10^{-16} , Invited talk at Int. Conf. on "Symmetries in Physics at Intermediate and High Energies and Applications", Ioannina-Greece, Sept. 30 - Oct. 5, 1998.
- [7] W. Molzon, The improved tests of muon and electron flavor symmetry in muon processes, Spring. Trac. Mod. Phys. **163** (2000)105.
- [8] T. Siiskonen, J. Suhonen, and T.S. Kosmas, Phys. Rev. **C 60** (Rapid Communication) (1999) 062501; Phys. Rev. **C**, submitted.
- [9] A. van der Schaaf, Prog. Part. Nucl. Phys. **B 31** (1993) 1; A. van der Schaaf, Private Communication.
- [10] C. Dohmen *et al.*, (SINDRUM II Collaboration), Phys. Lett. **B 317** (1993) 631.
- [11] W. Honecker *et al.*, (SINDRUM II Collaboration), Phys. Rev.Lett. **76** (1996) 200.
- [12] S. Ahmad *et al.*, (TRIUMF Collaboration), Phys.Rev.Lett. **59** (1987) 970.
- [13] T.S. Kosmas, J.D. Vergados, and A. Faessler, Phys. Atom. Nucl. **61** (1998) 1161.

- [14] H.C. Chiang, E. Oset, T.S. Kosmas, A. Faessler, and J.D. Vergados, Nucl. Phys. **A 559** (1993) 526.
- [15] T.S. Kosmas, A. Faessler and J.D. Vergados, J. Phys. **G 23** (1997) 693; J. Schwieger, T.S. Kosmas, and A. Faessler, Phys. Lett. **B 443** (1998) 7; T.S. Kosmas, Z. Ren and A. Faessler, Nucl Phys. **A 665** (2000) 183.
- [16] T.S. Kosmas and J.D. Vergados, Nucl. Phys. **A 510** (1990) 641.
- [17] J.E. Kim, P. Ko, and D.-G. Lee, Phys. Rev. **D 56** (1997) 100, hep-ph/9701381.
- [18] K. Huitu, J. Maalampi, M. Raidal, and A. Santamaria, Phys. Lett. **B 430** (1998) 355, hep-ph/9712249.
- [19] A. Faessler, T.S. Kosmas, S. Kovalenko, and J.D. Vergados, hep-ph/9904335.
- [20] R. Barbieri and L. Hall, Phys. Lett. **B 338** (1994) 212; R. Barbieri, L. Hall, and A. Strumia, Nucl. Phys. **B 445** (1995) 219.
- [21] L. Hall and M. Suzuki, Nucl. Phys. **B 231** (1984) 419; K. Enqvist, A. Masiero, A. Riotto, Nucl. Phys. **B 373** (1992) 95; H.-P. Nilles and N. Polonsky, Nucl. Phys. **B 484** (1997) 33; T. Banks, Y. Grossman, E. Nardi and Y. Nir, Phys. Rev. **D 52** (1995) 5319; E. Nardi, Phys. Rev. **D 55** (1997) 5772; F. de Campos, M.A. García-Jareño, A.S. Joshipura, J. Rosiek, and J.W.F. Valle, Nucl. Phys. **B 451** (1995) 3; F.M. Borzumati, Y. Grossman, E. Nardi, and Y. Nir, Phys. Lett. **B 384** (1996) 123.
- [22] G. Bhattacharyya, Nucl. Phys. Proc. Suppl. 52 A (1997) 83, IFUP-TH 43/97, hep-ph/9709395; H. Dreiner, in Proc. of *Perspectives on Supersymmetry*, Ed. by G.L. Kane, World Scientific, 462 (1999); P. Roy, Plenary talk given at the *Pacific Particle Physics Phenomenology Conference*, Seoul, Korea, Oct. 31 - Nov. 2, 1997, hep-ph/9712520; R. Barbier et al. Report of the GDR working group on the R-parity violation, hep-ph/9810232.
- [23] M. Nowakowski and A. Pilaftsis, Nucl. Phys. **B 461** (1996) 19; A. Joshipura and M. Nowakowski, Phys. Rev. **D 51** (1995) 2421.
- [24] A. Faessler, S. Kovalenko, and F. Šimkovic, Phys. Rev. **D 57** (1998) 055004.
- [25] H.-P. Nilles, Phys. Rep. **110** (1984) 1; H. Haber and G. Kane, Phys. Rep. **117** (1985) 75.
- [26] A. Faessler, S. Kovalenko, F. Šimkovic, and J. Schwieger, Phys. Rev. Lett. **78** (1997) 183; A. Faessler, S. Kovalenko, and F. Simkovic, Phys. Rev. **D 58** (1998) 11500, hep-ph/9803253.
- [27] J. Ashman *et al.*, EMC collaboration, Nucl. Phys. **B 328** (1989) 1.
- [28] G. Mallot, Nucl. Phys. **B 441** (1995) 12.
- [29] A. Manohar and R. Jaffe, Nucl. Phys. **B 337** (1990) 509.

- [30] M.A. Shifman A.I. Vainshtein and V.I. Zakharov, Phys. Lett. **B 78** (1978) 443.
- [31] T.P. Cheng, Phys. Rev. **D 38** (1988) 2869; H.-Y. Cheng, Phys. Lett. **B 219** (1989) 347; Phys. Lett. **B 317** (1993) 631.
- [32] H. de Vries, C.W. de Jager and C. de Vries, Atomic Data and Nuclear Data Tables, **36** (1987) 495.
- [33] W.R. Gibbs and B.F. Gibson, Ann. Rev. Nucl. Part. Sci. **37** (1987) 411; C. Garcia-Recio, J. Nieves and E. Oset, Nucl. Phys. **A 547** (1992) 473.
- [34] I.E. Lagaris, A. Likas, and D.I. Fotiadis, Comp. Phys. Commun. **104** (1997) 1.
- [35] T. Suzuki, *et al.*, Phys. Rev. **C 35** (1987) 2212.
- [36] V.A. Bednyakov, A. Faessler, and S. Kovalenko, Phys. Lett. **B 442** (1998) 203.
- [37] S. Lola and J. D. Vergados, Prog. Part. Nucl. Phys. **40** (1998) 71.
- [38] P. Binétruy, S. Lavignac and P. Ramond, Nucl. Phys. **B477** (1996) 353; V. Ben-Hamo, Y. Nir, Phys. Lett. **B339** (1994) 77; G. Bhattacharyya, hep-ph/9707297; P. Binétruy, E. Dudas, S. Lavignac, and C. A. Savoy, Phys. Lett. **B422** (1998) 171; J. Ellis, S. Lola and G.G. Ross, CERN-TH/97-205; hep-ph/9803308; F.M. Borzumati, Y. Grossman, E. Nardi and Y. Nir, Phys. Lett. **B384** (1996) 123.
- [39] G.K. Leontaris and J. Rizos, Nucl. Phys. **B 667** (2000) 32; hep-ph/9909206.

| A | Z | $\phi(A,Z)$ | $\tilde{\phi}(A,Z)$ |
|------|-----|-------------|---------------------|
| 12. | 6. | 0.000 | 0.000 |
| 24. | 12. | 0.014 | 0.000 |
| 27. | 13. | 0.000 | -0.037 |
| 32. | 16. | 0.023 | 0.000 |
| 40. | 20. | 0.037 | 0.000 |
| 44. | 20. | -0.063 | -0.091 |
| 48. | 22. | -0.083 | -0.083 |
| 63. | 29. | -0.056 | -0.079 |
| 90. | 40. | -0.054 | -0.111 |
| 112. | 48. | -0.108 | -0.143 |
| 208. | 82. | -0.152 | -0.212 |
| 238. | 92. | -0.175 | -0.227 |

Table 1: The variation of the quantity ϕ of Eq. (33) through the periodic table. For comparison its approximate expression $\tilde{\phi} \approx (A - 2Z)/A$ is also shown.

| Nucleus | $ \mathbf{p}_e (fm^{-1})$ | $\epsilon_b (MeV)$ | $\Gamma_{\mu c} (\times 10^6 s^{-1})$ | $\mathcal{M}_p (fm^{-3/2})$ | $\mathcal{M}_n (fm^{-3/2})$ |
|------------|----------------------------|--------------------|---------------------------------------|-----------------------------|-----------------------------|
| ^{27}Al | 0.531 | -0.470 | 0.71 | 0.047 | 0.045 |
| ^{48}Ti | 0.529 | -1.264 | 2.60 | 0.104 | 0.127 |
| ^{208}Pb | 0.482 | -10.516 | 13.45 | 0.414 | 0.566 |

Table 2: Transition matrix elements (muon-nucleus overlap integrals $\mathcal{M}_{p,n}$ of Eq. (34)) evaluated by using the exact muon wave function obtained via neural networks techniques. Other useful quantities (see text) are also included.

| Mechanism | ^{27}Al | ^{48}Ti | ^{208}Pb |
|---|------------------|------------------|-------------------|
| Photonic (γ) | 4.3 | 9.4 | 17.3 |
| W-boson exchange (γ) | 34.2 | 25.3 | 49.2 |
| SUSY s-leptons (γ) | 11.3 | 25.6 | 49.5 |
| SUSY Z-exchange (γ) | 27.6 | 110.6 | 236.2 |
| \mathcal{R}_p SUSY ($\gamma_{\mathcal{R}_p}$) | 16.5 | 46.4 | 96.9 |

Table 3: The nuclear physics part of the branching ratio $R_{\mu e}$, i.e. values of the function $\gamma_{\mathcal{R}_p}, \gamma$ of Eq. (38) for the nuclear targets ^{27}Al , ^{48}Ti and ^{208}Pb .

| Mechanism | ^{27}Al | ^{48}Ti | ^{208}Pb |
|----------------------|---------------------------------------|---------------------------------------|---------------------------------------|
| Photonic | $\rho \leq 4.6 \times 10^{-18}$ | $\rho \leq 8.2 \times 10^{-14}$ | $\rho \leq 3.2 \times 10^{-12}$ |
| W-boson exchange | $\rho \leq 5.8 \times 10^{-19}$ | $\rho \leq 3.0 \times 10^{-14}$ | $\rho \leq 1.1 \times 10^{-12}$ |
| SUSY sleptons | $\rho \leq 1.8 \times 10^{-18}$ | $\rho \leq 3.0 \times 10^{-14}$ | $\rho \leq 1.1 \times 10^{-12}$ |
| SUSY Z-exchange | $\rho \leq 7.3 \times 10^{-19}$ | $\rho \leq 0.7 \times 10^{-14}$ | $\rho \leq 0.2 \times 10^{-12}$ |
| \mathcal{R}_p SUSY | $\mathcal{Q} \leq 2.6 \cdot 10^{-19}$ | $\mathcal{Q} \leq 0.7 \cdot 10^{-14}$ | $\mathcal{Q} \leq 1.1 \cdot 10^{-13}$ |

Table 4: Experimental limits on the elementary particle sector of the exotic $\mu - e$ conversion. Quantities ρ and \mathcal{Q} are defined in of Eqs. (37) and Eq. (33), respectively. The limits are extracted from the recent experimental data for the nuclear targets ^{48}Ti and ^{208}Pb [10, 11] and from the expected sensitivity of the MECO experiment for the ^{27}Al target [6][see Eqs. (3)-(5)].

| Parameters | Previous limits | Present results $^{48}\text{Ti}(\mu - e) \cdot B_{Ti}$ | Expected results $^{27}\text{Al}(\mu - e) \cdot B_{Al}$ |
|-----------------------------------|-----------------------|---|--|
| $ \lambda'_{211} \lambda'_{111} $ | $4.4 \cdot 10^{-6}$ | $6.2 \cdot 10^{-8}$ | $4.0 \cdot 10^{-10}$ |
| $ \lambda'_{212} \lambda'_{112} $ | $4.4 \cdot 10^{-6}$ | $1.7 \cdot 10^{-8}$ | $1.1 \cdot 10^{-10}$ |
| $ \lambda'_{213} \lambda'_{113} $ | $4.4 \cdot 10^{-6}$ | $1.7 \cdot 10^{-8}$ | $1.1 \cdot 10^{-10}$ |
| $ \lambda'_{221} \lambda'_{111} $ | $1.5 \cdot 10^{-5}$ | $7.6 \cdot 10^{-8}$ | $4.9 \cdot 10^{-10}$ |
| $ \lambda'_{222} \lambda'_{112} $ | $1.5 \cdot 10^{-5}$ | $7.6 \cdot 10^{-8}$ | $4.9 \cdot 10^{-10}$ |
| $ \lambda'_{223} \lambda'_{113} $ | $1.5 \cdot 10^{-5}$ | $7.6 \cdot 10^{-8}$ | $4.9 \cdot 10^{-10}$ |
| $ \lambda'_{231} \lambda'_{111} $ | $[8.8 \cdot 10^{-5}]$ | $8.3 \cdot 10^{-6}$ | $5.3 \cdot 10^{-8}$ |
| $ \lambda'_{232} \lambda'_{112} $ | $4.8 \cdot 10^{-4}$ | $8.3 \cdot 10^{-6}$ | $5.3 \cdot 10^{-8}$ |
| $ \lambda'_{233} \lambda'_{113} $ | $4.8 \cdot 10^{-4}$ | $8.3 \cdot 10^{-6}$ | $5.3 \cdot 10^{-8}$ |
| $ \lambda'_{211} \lambda'_{121} $ | $3.0 \cdot 10^{-5}$ | $7.6 \cdot 10^{-8}$ | $4.9 \cdot 10^{-10}$ |
| $ \lambda'_{212} \lambda'_{122} $ | $3.0 \cdot 10^{-5}$ | $7.6 \cdot 10^{-8}$ | $4.9 \cdot 10^{-10}$ |
| $ \lambda'_{213} \lambda'_{123} $ | $3.0 \cdot 10^{-5}$ | $7.6 \cdot 10^{-8}$ | $4.9 \cdot 10^{-10}$ |
| $ \lambda'_{221} \lambda'_{121} $ | $8.0 \cdot 10^{-6}$ | $1.4 \cdot 10^{-8}$ | $9.0 \cdot 10^{-11}$ |
| $ \lambda'_{222} \lambda'_{122} $ | $8.0 \cdot 10^{-6}$ | $3.3 \cdot 10^{-7}$ | $2.1 \cdot 10^{-9}$ |
| $ \lambda'_{223} \lambda'_{123} $ | $8.0 \cdot 10^{-6}$ | $3.3 \cdot 10^{-7}$ | $2.1 \cdot 10^{-9}$ |
| $ \lambda'_{231} \lambda'_{121} $ | $1.6 \cdot 10^{-4}$ | $3.7 \cdot 10^{-5}$ | $2.4 \cdot 10^{-7}$ |
| $ \lambda'_{232} \lambda'_{122} $ | $1.6 \cdot 10^{-4}$ | $3.7 \cdot 10^{-5}$ | $2.4 \cdot 10^{-7}$ |
| $ \lambda'_{233} \lambda'_{123} $ | $1.6 \cdot 10^{-4}$ | $3.7 \cdot 10^{-5}$ | $2.4 \cdot 10^{-7}$ |
| $ \lambda'_{211} \lambda'_{131} $ | $[4.2 \cdot 10^{-4}]$ | $8.3 \cdot 10^{-6}$ | $5.3 \cdot 10^{-8}$ |
| $ \lambda'_{212} \lambda'_{132} $ | $4.8 \cdot 10^{-4}$ | $8.3 \cdot 10^{-6}$ | $5.3 \cdot 10^{-8}$ |
| $ \lambda'_{213} \lambda'_{133} $ | $[1.2 \cdot 10^{-5}]$ | $8.3 \cdot 10^{-6}$ | $5.3 \cdot 10^{-8}$ |
| $ \lambda'_{221} \lambda'_{131} $ | $1.6 \cdot 10^{-4}$ | $3.7 \cdot 10^{-5}$ | $2.4 \cdot 10^{-7}$ |
| $ \lambda'_{222} \lambda'_{132} $ | $1.6 \cdot 10^{-4}$ | $3.7 \cdot 10^{-5}$ | $2.4 \cdot 10^{-7}$ |
| $ \lambda'_{223} \lambda'_{133} $ | $[1.2 \cdot 10^{-5}]$ | $3.7 \cdot 10^{-5}$ | $2.4 \cdot 10^{-7}$ |
| $ \lambda'_{231} \lambda'_{131} $ | $3.5 \cdot 10^{-5}$ | $1.3 \cdot 10^{-8}$ | $8.3 \cdot 10^{-11}$ |
| $ \lambda'_{232} \lambda'_{132} $ | $3.5 \cdot 10^{-5}$ | $4.0 \cdot 10^{-3}$ | $2.6 \cdot 10^{-5}$ |
| $ \lambda'_{233} \lambda'_{133} $ | $3.5 \cdot 10^{-5}$ | $4.0 \cdot 10^{-3}$ | $2.6 \cdot 10^{-5}$ |

Table 5: Upper bounds on $\lambda'_{ijk} \lambda'_{lmn}$ derived in the tree-level \mathcal{R}_p SUSY mechanism from the SINDRUM II data on the $\mu^- - e^-$ conversion in ^{48}Ti [Eq. (3)] and from the expected sensitivity [Eq. (5)] of the MECO experiment at BNL with ^{27}Al . For comparison we present previous bounds derived in the 1-loop \mathcal{R}_p SUSY mechanism [18]. In brackets [] we show bounds from the other processes (for references see Refs. [22, 18]) when they are more stringent than the 1-loop $\mu^- - e^-$ conversion bounds. The limits are given for the scalar superpartner masses $\tilde{m} = 100$ GeV. The scaling factor B is defined in Eq. (41).

| Parameters | Previous limits | Present results $^{48}\text{Ti}(\mu - e) \cdot B_{Ti}$ | Expected results $^{27}\text{Al}(\mu - e) \cdot B_{Al}$ |
|----------------------------------|---------------------|---|--|
| $ \lambda'_{211} \lambda_{212} $ | $4.5 \cdot 10^{-3}$ | $4.1 \cdot 10^{-9}$ | $2.6 \cdot 10^{-11}$ |
| $ \lambda'_{311} \lambda_{312} $ | $6.0 \cdot 10^{-3}$ | $4.1 \cdot 10^{-9}$ | $2.6 \cdot 10^{-11}$ |
| $ \lambda'_{111} \lambda_{121} $ | $1.5 \cdot 10^{-5}$ | $4.1 \cdot 10^{-9}$ | $2.6 \cdot 10^{-11}$ |
| $ \lambda'_{311} \lambda_{321} $ | $6.0 \cdot 10^{-3}$ | $4.1 \cdot 10^{-9}$ | $2.6 \cdot 10^{-11}$ |
| $ \lambda'_{222} \lambda_{212} $ | $9.0 \cdot 10^{-3}$ | $7.7 \cdot 10^{-9}$ | $5.0 \cdot 10^{-11}$ |
| $ \lambda'_{322} \lambda_{312} $ | $1.2 \cdot 10^{-2}$ | $7.7 \cdot 10^{-9}$ | $5.0 \cdot 10^{-11}$ |
| $ \lambda'_{122} \lambda_{121} $ | $1.0 \cdot 10^{-3}$ | $7.7 \cdot 10^{-9}$ | $5.0 \cdot 10^{-11}$ |
| $ \lambda'_{322} \lambda_{321} $ | $1.2 \cdot 10^{-2}$ | $7.7 \cdot 10^{-9}$ | $5.0 \cdot 10^{-11}$ |

Table 6: The same as in Table 5 but for the upper bounds on $\lambda'_{ijk}\lambda_{lmn}$. Previous limits are taken from the other processes (for references see Refs. [22, 18]). The 1-loop \mathcal{R}_p SUSY mechanism [18] does not constraint these products of the \mathcal{R}_p couplings.